Meteorologische Zeitschrift, Vol. **16**, No. 6, 1-10 (December 2007)

Article

Increasing the Atlantic subtropical jet cools the circum-North Atlantic Region

G. VAN DER SCHRIER*[1], S.S. DRIJFHOUT[1], W. HAZELEGER[1] and L. NOULIN[2]

[1]Royal Netherlands Meteorological Institute, De Bilt, The Netherlands
[2] Ecole d'Ingénieurs en Modélisation Mathématique et Mécanique, Talence, France

(Manuscript received February 6, 2007; in revised form July 13, 2007; accepted October 19, 2007)

Abstract

The aim of this paper is to model part of a scenario for abrupt climate change over the North Atlantic sector in a General Circulation Model of intermediate complexity. Central to this scenario is the hypothesis that a substantial strengthening of the Atlantic subtropical jet will lead to a reorganization of the mid-latitude atmospheric circulation in which the Atlantic subtropical and eddy-driven jets coincide. The subtropical jet over the North Atlantic sector is increased by calculating optimal model tendency perturbations, using a recently developed technique. Strengthening of the subtropical jet is achieved by model tendency perturbations which (1) sharpen the meridional gradient in streamfunction or (2) force a strong and persistently negative North Atlantic Oscillation pattern in the upper troposphere. Both approaches lead to similar forcing patterns. It is found that when the subtropical jet is sufficiently strong, the eddy-driven jet is indeed drawn to the northern rim of the subtropical jet. This reduces atmospheric meridional heat transport over the North Atlantic. In the model, a positive feedback is observed; the southern sea ice-edge extends further south and snowcover over Europe is more persistent. All factors combined result in an overall cooling of the circum-North Atlantic region.

Zusammenfassung

In einem Allgemeineen Zirkulationsmodell mittlerer Komplexität wird ein Teil eines Szenariums für einen plötzlichen Klimawandel im Nordatlantischen Gebiet modelliert. Die Basishypothese dieses Szenariums ist dass eine deutliche Verstärkung des subtropischen Jets über dem Atlantik zu einer Veränderung der atmosphärischen Zirkulation in den mittleren Breiten führt, bei der der subtropische und der wirbelgetriebene Jet zusammenfallen.
Der subtropische Jet über dem Nordatlantik wird verstärkt indem mit einer kürzlich entwickelten Methode optimale Störungen der Modelltendenzen berechnet werden. Eine Verstärkung des subtropischen Jets wird durch Störungen der Modelltendenzen erreicht, die (1) den meridionalen Gradienten der Stromfunktion erhöen, oder (2) das Modell bleibend in ein Strömungsmuster drängen, dass der negativen Phase der Nordatlantischen Oszillation in der oberen Troposphäre entspricht.
Beide Ansäze führen zu denselben antreibenden Mustern. Wir finden dass ein genügend starker subtropischer Jet tatsächlich dazu führt, dass der wirbelgetriebene Jet in den nördlichen Rand des subtropischen Jets gezogen wird. Dies vermindert den meridionalen atmosphärischen Wärmetransport über dem Nordatlantik. Im Modell wird eine positive Rückkopplung beobachtet: Die südliche Grenze des Meereises verschiebt sich nach Süden, und Europa bleibt länger schneebedeckt. Alle Faktoren zusammen führen zu einer Abkühlung des Nordatlantischen Gebietes.

1 Introduction

Paleoclimatic reconstructions of climate parameters, covering the timespan from the end of the last glacial period to present times, are punctuated with brief, but wide-spread, transitions to a colder climate. The rapid transitions occur on timescales much shorter than any expected change in external forcing (TAYLOR et al., 1993; GRIPMEMBERS, 1993). These observations have led to the concept that abrupt climate changes need a trigger, an amplifier and a globalizer (HOSKINS, 2003) to explain their sudden, near-instant and global or hemispheric-wide impact. The triggers and amplifiers for abrupt climate changes like the Younger Dryas event, at the transition between the last glacial to the present interglacial at ca. 11 kyr BP, or the 8.2ka cooling event have generally been thought of as residing in the coupled land-ice/ocean system. Massive outflows of glacial meltwater from the Laurentide icesheet would dilute the waters of the northern North Atlantic to the point that deep convection, essential for maintaining the Meridional Overturning Circulation (MOC), would be halted. With convection and the MOC stopped, oceanic heat transport would reduce drastically, plunging the circum-Atlantic region into a much cooler climate.

Recently, this hypothesis has been challenged. For the Younger Dryas, the freshwater route from Lake Agassiz, in which the meltwater accumulated, to the

*Corresponding author: G. van der Schrier, KNMI, PO BOX 201 3730 AE, De Bilt, The Netherlands, e-mail: schrier@knmi.nl

0941-2948/2007/0252 $ 4.50
DOI: 10.1127/0941-2948/2007/0252

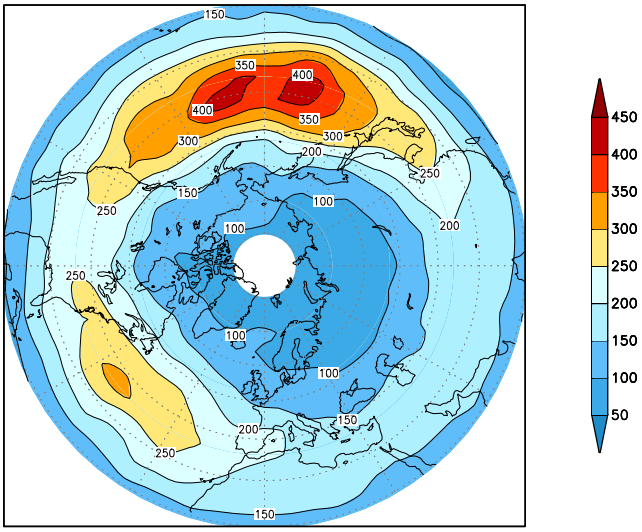

Figure 1: Transient eddy kinetic energy (m^2 s^{-2}) at 200hPa, averaged over December-February, in the ECBilt model.

North Atlantic ocean remains unknown (BROECKER, 2006), casting doubt on the suggested massive melt water flux which was thought to preceed this phase. Moreover, for the 8.2ka event, geologic evidence has been found for a meltwater pulse into the North Atlantic, but it predates the cooling event by some 200-300 years (ROHLING and PÄLIKE, 2005). This makes it less likely that a meltwater pulse triggered this event.

An alternative hypothesis on the trigger of rapid climate change involves an active role for the atmosphere and hinges on the repositioning of the Atlantic eddy-driven jet to a more zonal position. The Atlantic storm track and subpolar, or eddy-driven jet have a clear southwest - northeast path way (HOSKINS and VALDES, 1990) and are largely responsible for mid-latitude meridional heat transport (TRENBERTH and CARON, 2001). If the Atlantic eddy-driven jet would have a more zonal track, the North Atlantic region and western Europe would be devoid of the heat brought by the southerly flows, which was shown to be essential for Europe's mild winters (SEAGER et al., 2002). The strongly reduced atmospheric meridional heat transport would lead to large-scale changes in North Atlantic sea-ice cover and subsequently to changes in the surface and deep Atlantic ocean circulation, amplifying the cooling (SEAGER and BATTISTI, 2007). Recent results (LEE and KIM, 2003) show that with a sufficiently strong subtropical jet, the primary region of baroclinic wave growth would shift from the mid-latitude eastern seaboard of America to the north side of this jet. In the hypothesis, the eddy-driven jet would be drawn to the northern edge of the subtropical jet when the latter is of sufficient strength, leading to the reorganization of atmospheric circulation.

The present study aims to model a climate in a coupled ocean-atmosphere-sea ice model in which the eddy driven jet over the North Atlantic sector has collapsed unto the northern rim of the subtropical jet. We expect to achieve the reorganization of mid-latitude atmospheric circulation by a substantial increase in the strength of the subtropical jet. A more vigorous subtropical jet is in its turn achieved by calculating optimal tendency perturbations to the atmospheric core of the GCM. The intent of this exercise is to investigate if the proposed chain-of-events leading to a harsher North Atlantic climate can be reproduced in a climate model; an experiment not conducted before. In this study, we only suggest possible dynamical origins of the applied tendency perturbations and refrain from making the source of these perturbations more explicit. In that sense, the experimental setup in this study is similar to the common 'hosing' experiments (e.g. VELLINGA and WOOD, 2002). In these experiments, an artificial source of fresh water is added to the North Atlantic ocean, suggestive of meltwater inflow, in order to perturb the Atlantic's Meridional Overturning Circulation.

2 Model description

The model, ECBilt-Clio, is a coupled ocean-atmosphere-sea ice general circulation model of intermediate complexity (OPSTEEGH et al., 1998; GOOSSE and FICHEFET, 1999). The atmospheric component (ECBilt) is a spectral T21 (L3) quasi-geostrophic model with simplified parameterizations for the diabatic processes. The three levels are at 800 hPa, 500 hPa and 200 hPa. The dynamical component was developed by Molteni (MARSHALL and MOLTENI, 1993). The physical parameterizations are similar to those by HELD and SUAREZ (1978). An estimate of the neglected ageostrophic terms in the vorticity and thermodynamic equations has been added to the quasi-geostrophic model as a time and spatially varying forcing. This forcing is computed from the diagnostically derived vertical motion field. With the inclusion of the ageostrophic terms, the model simulates the Hadley circulation qualitatively correct. This results in an improvement of the strength and position of the jet stream and transient eddy activity. With a T21 resolution, not all waves which might become baroclinically unstable are resolved, but the model does show baroclinic instability. This leads us to conclude that the essentials of baroclinic instability are included, but the variability associated with it is underestimated compared to modern observations.

The transient eddy activity of the ECBilt model at the 200hPa level, a December-February average, is shown in Fig. 1. It shows a similar pattern as the 90-day low-pass filtered transient eddy kinetic

energy at 250 hPa as shown in the ERA-40 atlas (available online at www.ecmwf.int/research/era/ERA-40_Atlas/index.html). Similar to the reanalysis, the model shows a maximum in transient eddy activity over the western Pacific and a secondary maximum over eastern North America and the western Atlantic. The main differences with the reanalysis atlas are the strong underestimation of the eddy variability in the model, about a factor three over the Atlantic, and that the model's maxima in transient eddy kinetic energy are positioned too far north. The double-jet structure over the Atlantic sector is less pronounced in the model than in the reanalysis. The simplified nature and coarse resolution of the atmosphere model explain the low eddy-variability and weak zonal winds associated with the jet (OPSTEEGH et al., 1998).

The oceanic component (Clio) is a primitive equation, free-surface ocean general circulation model coupled to a thermodynamic-dynamic sea ice model and includes a relatively sophisticated parameterization of vertical mixing (GOOSSE et al., 1999). A three-layer sea-ice model, which takes into account sensible and latent heat storage in the snow-ice system, simulates the changes of snow and ice thickness in response to surface and bottom heat fluxes. The simulated position of the Arctic sea-ice edge in both winter and summer is in good agreement with observations (GOOSSE et al., 2002). The horizontal resolution of Clio is $3^\circ \times 3^\circ$ and it has 20 unevenly spaced layers in the vertical.

This simplified GCM has been used earlier in a broad range of studies, from ocean-atmosphere interaction (SELTEN et al., 1999) to numerous paleoclimatic studies (http://www.knmi.nl/onderzk/CKO/ecbilt-papers.html).

3 Forcing the subtropical jet

3.1 Forced sensitivity calculations

In sensitivity calculations which are operational at Numerical Weather Prediction agencies, the goal is to find *a posteriori* analysis perturbations that result in a modified model-atmosphere. These analysis perturbations are optimized to improve the forecast. Here we search for tendency perturbations rather than analysis perturbations, to modify the model-atmosphere. The tendency perturbations are optimized to lead to a stronger subtropical jet over the North Atlantic sector.

These tendency perturbations are referred to as *forcing singular vectors* (BARKMEIJER et al., 2003) and can be computed using an adjoint model (LACARRA and TALAGRAND, 1988). This technique has earlier been applied in a paleoclimatic setting by VAN DER SCHRIER and BARKMEIJER (2005, 2007). The tendency perturbations are used to modify large-scale patterns of variability only, leaving the synoptic scale variability to evolve freely. A detailed description of forcing singular vectors is given elsewhere (BARKMEIJER et al., 2003), here we give a brief outline only.

The prognostic variable in the dynamic part of the ECBilt model is potential vorticity, which can be related, through the linear balance equation, to streamfunction. In the following we will focus on streamfunction. The streamfunction $\psi(t,\mathbf{x})$ at time t is written as a superposition of the climatological mean $\psi_{\rm clim}(\mathbf{x})$ plus variability, written as an orthogonal expansion in basis functions $\psi_n(\mathbf{x})$:

$$\psi(t,\mathbf{x}) = \psi_{\rm clim}(\mathbf{x}) + \alpha(t)\psi_{\rm target}(\mathbf{x}) + \sum_{n=2} \alpha_n(t)\psi_n(\mathbf{x}). \tag{3.1}$$

The first basis function is the so-called target pattern $\psi_{\rm target}(\mathbf{x})$, with $\alpha(t)$ the projection coefficient of the model atmosphere on the target pattern. We are interested in tendency perturbations $\mathbf{f}$ that will produce, after some integration time T, or an optimization time, a deflection of the model atmospheric state in the direction of the target pattern. The amplitude of this deflection is $1-\alpha(t)$ times the amplitude of the target pattern, and makes that the projection of the target pattern on the deviation of model state from climatology is one. In short, given at $t = t_0$:

$$< \psi(t_0,\mathbf{x}) - \psi_{\rm clim}(\mathbf{x}), \psi_{\rm target}(\mathbf{x}) >= \alpha(t_0),$$

we aim to have:

$$< \psi(t_0+T,\mathbf{x}) - \psi_{\rm clim}(\mathbf{x}), \psi_{\rm target}(\mathbf{x}) >= 1.$$

The variability of the model which is orthogonal to the target pattern is captured in the expansion $\sum_{n=2} \alpha_n(t)\psi_n(\mathbf{x})$ and remains unaffected.

If the tendency perturbations are sufficiently small, the evolution of deviations of the model atmospheric state which results from tendency perturbations can be computed by a linearization of the GCM along a (time-dependent) solution of this GCM. The linear evolution of a perturbation ε, measuring the deviation between a control and perturbed model run, satisfies:

$$\frac{\mathrm{d}\varepsilon}{\mathrm{d}t} = \mathbf{L}\varepsilon + \mathbf{f}, \tag{3.2}$$

where $\mathbf{L}$ is the time dependent linearization of the GCM along a solution. Solutions of equation (3.2) take the form:

$$\varepsilon(T) = \mathbf{M}(0,T)\varepsilon(0) + \int_0^T \mathbf{M}(s,T)\mathbf{f}\mathrm{d}s, \tag{3.3}$$

where $\mathbf{M}(s,T)$ is the propagator from time s to time T of equation (3.2) without forcing: $\mathbf{f} = 0$. For an arbitrary forcing $\mathbf{f}$, the vector $\mathbf{y} = \mathscr{M}\mathbf{f}$, where

$$\mathscr{M} = \int_0^T \mathbf{M}(s,T)\mathrm{d}s, \tag{3.4}$$

is simply determined by integrating (3.2) to time $t = T$ with initial condition $\varepsilon(0) = 0$. Here $\mathbf{f}$ is constant over the optimization time T.

The forcing perturbation is now determined by minimization of:

$$J(\mathbf{f}) = \left| P\left(\mathscr{M}\mathbf{f} - (1-\alpha)\psi_{\text{target}}\right)\right|. \qquad (3.5)$$

The operator P is a projection operator, and is used in this application to limit the evaluation of the cost function to the North Atlantic sector and at the 200 hPa level only. The norm used here to constrain $\mathbf{f}$ is a simple L_2-norm, but other norms can be used too. A fast and efficient minimization routine requires the derivative of (3.5) with respect to $\mathbf{f}$, which can be efficiently computed using the adjoint of $\mathscr{M}$.

The gradient of $J(\mathbf{f})$, required in the quasi-Newton conjugate gradient method (NAG's E04DGF), is:

$$\nabla J = 2\mathscr{M}^* P^* P\left(\mathscr{M}\mathbf{f} - (1-\alpha)\psi_{\text{target}}\right) \qquad (3.6)$$

To derive the adjoint of $\mathscr{M}$ it is instructive to write (3.2) as:

$$\frac{\mathrm{d}}{\mathrm{d}t}\begin{pmatrix}\varepsilon\\ \mathbf{f}\end{pmatrix} = \begin{pmatrix}\mathbf{L} & \mathbf{I}\\ \mathbf{0} & \mathbf{0}\end{pmatrix}\begin{pmatrix}\varepsilon\\ \mathbf{f}\end{pmatrix}, \qquad (3.7)$$

where $\mathbf{I}$ and $\mathbf{0}$ are the identity and zero operator respectively. The adjoint of (3.7) is:

$$-\frac{\mathrm{d}}{\mathrm{d}t}\begin{pmatrix}\hat{\varepsilon}\\ \hat{\mathbf{f}}\end{pmatrix} = \begin{pmatrix}\mathbf{L}^* & \mathbf{0}\\ \mathbf{I} & \mathbf{0}\end{pmatrix}\begin{pmatrix}\hat{\varepsilon}\\ \hat{\mathbf{f}}\end{pmatrix}. \qquad (3.8)$$

By writing (3.8) as a coupled system again:

$$-\frac{\mathrm{d}}{\mathrm{d}t}\hat{\varepsilon} = \mathbf{L}^*\hat{\varepsilon} \qquad (3.9a)$$

$$-\frac{\mathrm{d}}{\mathrm{d}t}\hat{\mathbf{f}} = \hat{\varepsilon} \qquad (3.9b)$$

it follows how to determine $\mathscr{M}^*\mathbf{y}$ for a given input vector $\mathbf{y}$. First: integrate the regular adjoint model as given by equation (3.9aa) backward in time $t = T$ to time $t = 0$, with $\hat{\varepsilon}(T) = \mathbf{y}$. Second: integrate equation (3.9ab) backward in time from time $t = T$ using the intermediate fields of the adjoint integration (3.9aa) as tendencies for the corresponding time step and $\hat{\mathbf{f}}(T) = 0$. Integrating to time $t = 0$ yields $\mathscr{M}^*\mathbf{y} = \hat{\mathbf{f}}(0)$.

A linearization of the dynamic core of the atmospheric part (ECBilt) and its adjoint exist. They have been used earlier in predictability studies (BARKMEIJER et al., 1993) and to produce prescribed flow regimes in a forecast (OORTWIJN and BARKMEIJER, 1995) and are used here too in the evaluation of the forcing perturbation $\mathbf{f}$. A linearization of the atmospheric physics of the model, including the parametrized processes, is not available and is therefore not included in the computation of $\mathbf{f}$. This is an accurate approximation if the optimization time T is sufficiently small.

In this study, the optimization time T has been set to 72 hours, which means that every 72 hours $\mathbf{f}$ is updated.

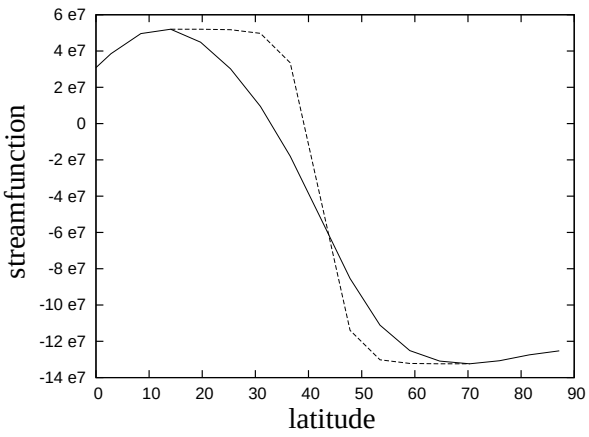

Figure 2: Example of the meridional structure of the streamfunction ($m^2\ s^{-1}$) at 200hPa (solid) for an arbitrary longitude. The dashed line shows the fit of the hyperbolic tangent to this graph, giving a sharper meridional gradient.

3.2 Sharpening the meridional gradient in ψ

Aiming to increase the strength of the subtropical jet over the North Atlantic sector, we calculated tendency perturbations which were optimized to sharpen the meridional gradient in the streamfunction ψ. On the rectangular latitude-longitude grid, an adjusted streamfunction is constructed by fitting a tangent hyperbolic between the maximum and minimum values the streamfunction attains in each latitudinal section within the North Atlantic sector. The adjusted streamfunction ψ_{adjusted} is constructed to have a steeper slope than the original streamfunction, without changing the position of the maximum slope in streamfunction. Fig. 2 shows an example of the original streamfunction and its adjusted version for one meridional section. An 'adjusted' streamfunction profile is calculated for every meridional section in the North Atlantic sector (ca. 90°W-40°E), which then span ψ_{adjusted}. The target pattern for this application is given by

$$\psi_{\text{target}} = \psi_{\text{adjusted}} - \psi. \qquad (3.10)$$

In a series of experiments, we determined the largest possible meridional gradient in ψ_{adjusted} which resulted in maximum values of the zonal velocity. Increasing the steepness of the gradient in ψ resulted in a saturation of the maximum zonal velocity. Averaged over December-February, the maximum zonally averaged zonal velocity we could reach with this approach in a 10-year simulation was 45.1 m/s, a considerable increase over to the 26.2 m/s of the control simulation. This is illustrated in Fig. 3, where the Jet Stream Index (JSI) (RUTI et al., 2006) is shown, calculated daily as the maximum of the zonal mean of the zonal wind at 200 hPa over the North-Atlantic sector. This experiment is referred to as EXP1. The tendency perturbations were applied

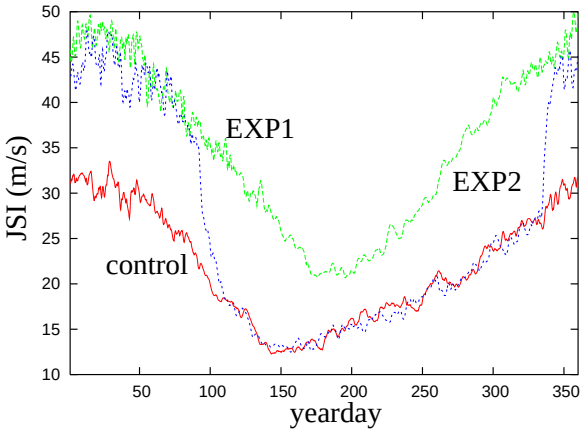

Figure 3: 10 years averaged daily values of the Jet Stream Index (JSI) of EXP1 (green) and EXP2 (blue) and the control simulation (red).

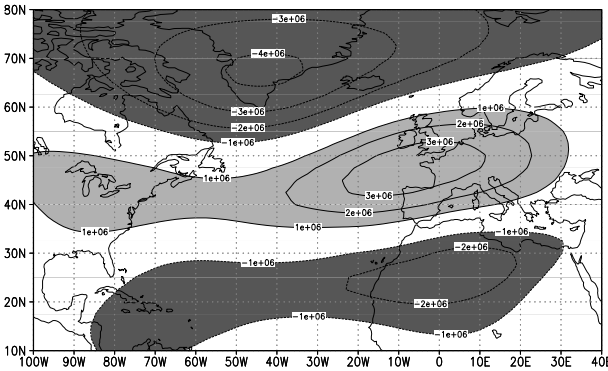

Figure 4: Regression of the December - March averaged NAO-index on 200hPa streamfunction ($m^2\ s^{-1}$).

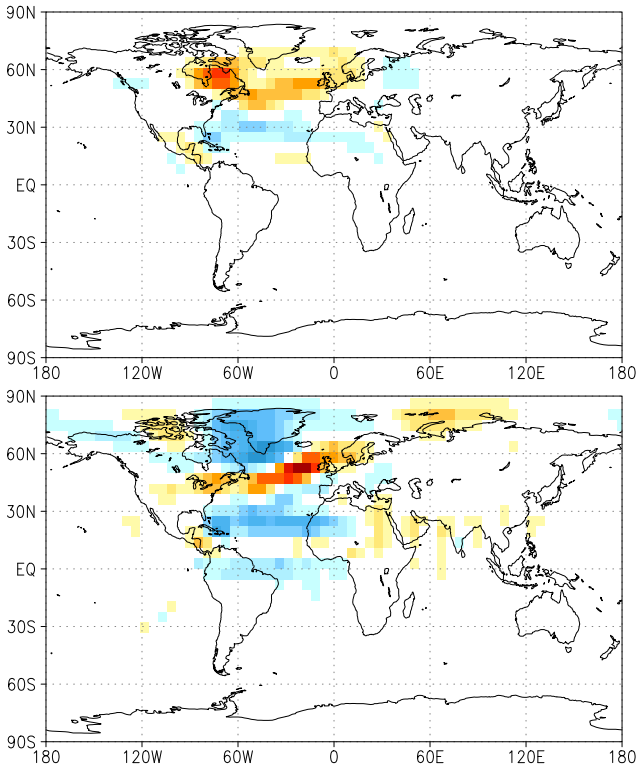

Figure 5: Mean model tendency perturbation at the 200hPa level for EXP1 (upper panel) and EXP2 (lower panel). Red and yellow colours denote positive values, blue colours denote negatve values. Values are in dimensionless units.

throughout the year, but we will analyze results from winter (December-February) only.

3.3 Forcing a persistently negative NAO

The NAO is the most dominant mode of atmospheric variability in boreal winter over the North Atlantic sector. An alternative approach to increase the strength of the subtropical jet, is to force a strong and persistently negative NAO-state on streamfunction at the 200hPa level. Fig. 4 shows the regression of the DJFM NAO-index (JONES et al., 1997) on 200hPa DJFM streamfunction fields of the NCEP/NCAR reanalysis. In a series of forced sensitivity experiments, we used this pattern as the target pattern and determined for which amplitude of the regression pattern shown in Fig. 4 we attained zonal wind speeds comparable to EXP1. This value turned out to be -5.

A second 10-year simulation was made with a persistently negative NAO state (averaged over DJFM) at index value -5, which we refer to as EXP2. We could reach the maximum zonally averaged zonal velocity with this approach of 43.3 m/s, again a considerable increase compared to the ca. 26 m/s of the control simulation (Fig. 3).

The approach outlined in § 3.1 will force the model atmosphere to the target pattern at, or near, the desired amplitude, while it leaves the atmosphere free to respond in a dynamically consistent way to any changes in climatic conditions. Importantly, synoptic-scale variability internal to the atmospheric or climatic system is not suppressed and can adjust to the changes in the large-scale atmospheric circulation.

In contrast to the approach in EXP1, tendency perturbations were applied in the December-March period only. No perturbations are applied in the remaining part of the year, which is reflected in the rapid return and quick spin-up to and from climatological mean jet-strength (Fig. 3). The differences in experimental setup between EXP1 and EXP2 are summarized in table 1.

Figure 5 shows the mean tendency perturbations **f** for EXP1 and EXP2 at the 200hPa level. The patterns of the mean tendency perturbations have some similarities, which is remarkable given the different approaches to strengthening the subtropical jet. The tendency perturbations of both experiments have their largest standard deviation over the Atlantic sector, with EXP2 having a temporal standard deviation which is consistently lower (ca 0.75 times) than that of EXP1. The main differences

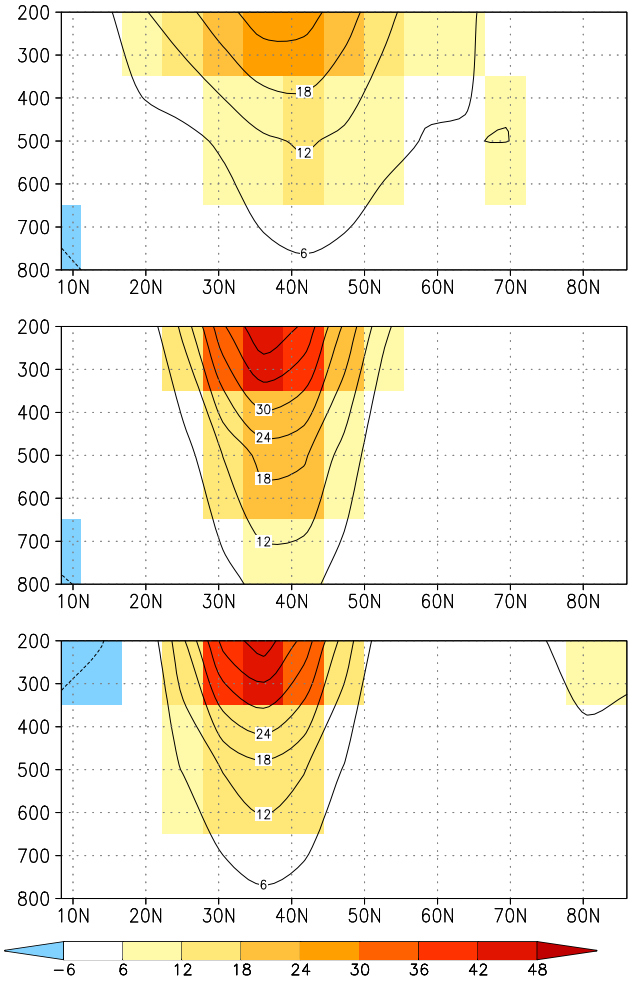

Figure 6: Zonally averaged zonal velocity (m s^{-1}) for the control simulation (Fig. a), EXP1 (Fig. b) and EXP2 (Fig. c). The zonal velocity is averaged over the North Atlantic sector (60°W,40°E) and averaged over the December-February period. Both contours and colourbar denote zonally averaged zonal velocity.

between the patterns is that the mean tendency perturbation of EXP2 has a larger amplitude than that of EXP1. The difference in mean and temporal standard deviation of the forcing patterns are related to the stationarity of the target pattern in EXP2, with only the time expansion coefficient $\alpha(t)$ (equation 3.1) changing when a new tendency perturbation is calculated. The spatial structure of the target pattern in EXP1 is related to changes in position and strength of meanders of the subtropical jet too, which explains the higher variance and lower mean of the forcing pattern of EXP1. On synoptic timescales, the model tendency perturbations in EXP1 and EXP2 are about equal.

4 Results

4.1 Changes in atmospheric circulation

Figure 6a shows the zonally averaged zonal velocity over the North Atlantic sector for DJF in the 200-yr control simulation. The 500hPa zonal wind velocity attains its maximum value at ca. 70°N. Due to the diffusive nature of the model, associated with the coarse resolution, a clearly separated eddy-driven jet is not present. The subtropical jets in EXP1 and EXP2 (Figs. 6b and c) averaged over DJF, are narrower than in the control simulation. Maximum zonal wind speeds are reached in all simulations between 30°N and 40°N. Although the subtropical jet at 200 hPa in EXP2 is far stronger than that of the control simulation, Fig. 6c shows that at the 800hPa level wind strengths are comparable. This is in contrast to EXP1, where strong winds are found at all vertical levels of the model.

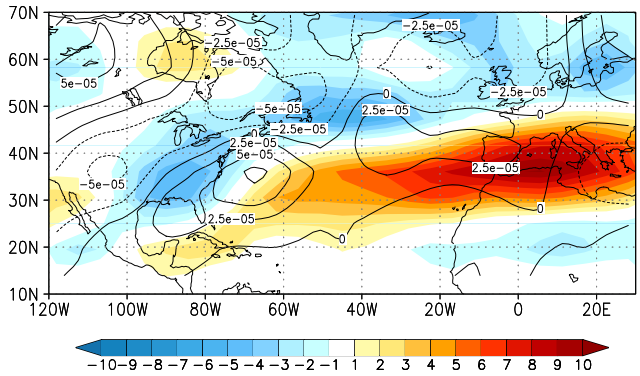

Figure 7: The change in zonal wind speed, averaged over December-February, for EXP2 (m s^{-1}, colors) and the change in horizontal divergence of the E-vector (m s^{-2}, contours).

A conspicuous aspect of Fig. 6 is that the maxima in zonal wind, associated with the eddy-driven jets, are absent in EXP1 and EXP2. This is confirmed in Fig. 7 which shows a strong weakening of the westerly eddy-driven jet and an increase in zonal windstrength at the northern rim of the subtropical jet at the 500hPa level. This figure also shows contours of the change in horizontal divergence of the E-vector, which is the generalization of the Eliassen-Palm flux to three-dimensional flow and associated with the eddy forcing of the mean flow (JAMES, 1994). The E-vector is diagnosed at every timestep of the model and recalculated into monthly averages. It shows a convergence of the E-vector, implying westerly deceleration, slightly north of the area with a reduction in zonal wind speed, and a divergence, implying westerly acceleration, somewhat north of the increase in zonal wind speed. The poleward shift in maxima/minima of E-vector divergence is consistent with observations (JAMES, 1994 [P.238]) and is attributed to other processes which act to generate the observed jets. The results of EXP1 and EXP2 are in agreement with those of LEE and KIM (2003), who found that as the subtropical jet strengthens, a transition occurs from a double jet situation, with the subtropical jet and eddy-driven jet coexisting, to a single jet situation. The mechanism identified for this transition is that a state with

a strong subtropical jet will have its primary region of baroclinic wave growth at the north side of the subtropical jet. This results in the formation of the eddy-driven jet just north of the subtropical jet, instead of at the mid-latitude baroclinic zone. Given the more zonal orientation of the subtropical jet, this makes that the position of the eddy-driven jet becomes more zonal too. This mechanism can also be identified in EXP1 and EXP2. Figure 8 shows the difference in maximum Eady growth rate at 650hPa (DJF averaged) between EXP1/EXP2 and the control simulation. This figure shows that the baroclinicity found in the control simulation from the east coast of the North American continent extending in northeasterly direction over the Atlantic strongly decreases in EXP1 and EXP2. Instead, highest values of the Eady growth rate are drawn to the south and align with the northern side of the subtropical jet in EXP1 and EXP2. Moreover, high values of the Eady growth rate for EXP1 and EXP2 are found in a zonal band over the Atlantic sector between ca. 35°N and 40°N. The Eady growth rates in EXP1 and EXP2 are ca. 1.3 to 1.4 times larger than in the control simulation.

4.2 Impact on climate

Motivated by the similarities in the behaviour of the subtropical and eddy-driven jet and in the tendency perturbations between EXP1 and EXP2, and for the sake of brevity, we restrict the description of the impact on climate in the North Atlantic sector to EXP2 only. Figure 9 shows that the reorganization of the eddy-driven jet in EXP2 has an impact in atmospheric meridional heat transport over the North Atlantic sector. This figure shows the ratio between atmospheric meridional heat transport (MHT) between EXP2 and the control simulation, averaged over the North Atlantic sector. MHT is higher in EXP2 with respect to the control climate for the latitudes in which we find the subtropical jet and it is much lower for the latitudes north of this, illustrating the relocation of the eddy-driven jet to a more southerly position.

The repositioning of the eddy-driven jet affects the sea-ice coverage of the North Atlantic ocean too. Figure 10 shows the increase in albedo for EXP2 for January-March, clearly indicating that the sea-ice fraction of the gridboxes on the southern rim of the sea-ice edge increases. Higher albedo is also found in western Europe which is related to a extended snow coverage over this area.

The decrease in atmospheric meridional heat transport seems to be slightly compensated by an increase in the oceanic meridional heat transport. In EXP2, the Meridional Overturning Circulation (MOC) increases slightly, explaining this increase in oceanic heat transport. However, the average position of deep-water formation shifts southward, releasing the heat associated

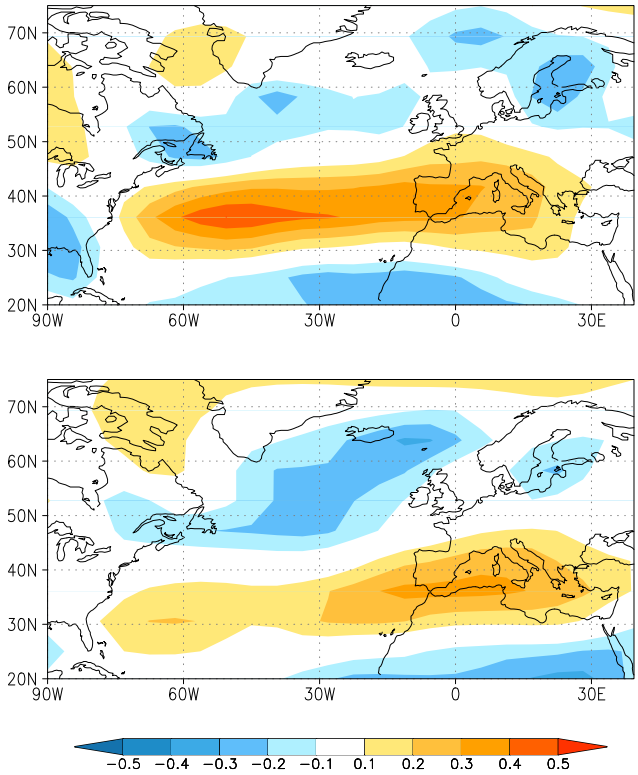

Figure 8: Maximum Eady growth rate (day^{-1}) at the 650hPa level as a deviation form the control simulation, averaged over DJF for EXP1 (upper panel) and for EXP2 (lower panel). Higher values of the Eady growth rate in EXP1 and EXP2 are found for the entire width of the North Atlantic sector between ca. 35°N and 40°N, just north of the latitude with maximum zonal windspeed. A decrease in Eady growth rate with respect to the control simulation is found along the path way of the control-simulation's eddy-driven jet, between 40°N and 70°N.

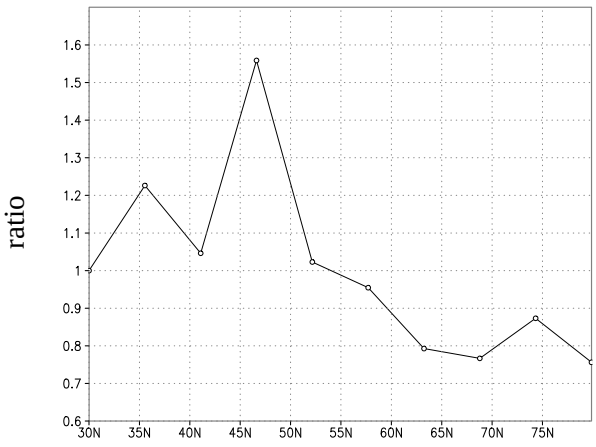

Figure 9: Ratio between atmospheric meridional heat transport in EXP2 and that of the control simulation, averaged over the North Atlantic sector (ca. 90°W-40°E).

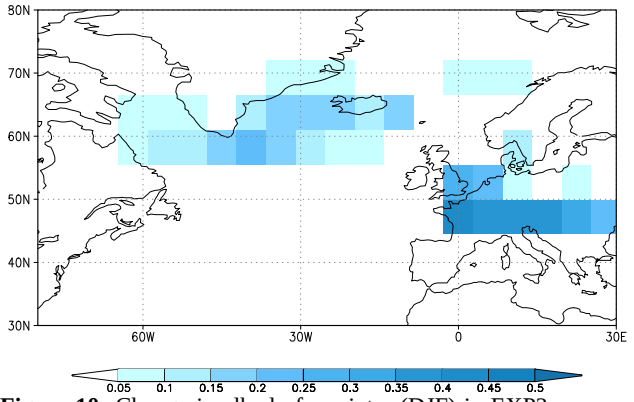

Figure 10: Change in albedo for winter (DJF) in EXP2 compared to the control simulation.

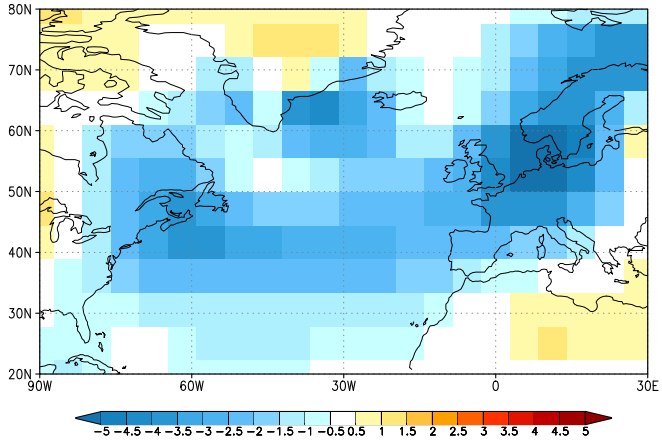

Figure 11: Change in surface air temperature (°C) for winter (DJF) in EXP2 compared to the control simulation.

with deep-water formation at lower latitudes. The shift in the main deep water formation site to a more southerly latitude is consistent with a southward spreading of sea-ice.

The results of EXP2 show a drastic change in winter surface air temperatures in response to the changes in atmospheric circulation and the increase in albedo. Fig. 11 shows the change in 2 m DJF-temperature with respect to the control climate, showing areas with a decrease in temperature reaching up to 5°C.

In EXP2, no tendency perturbations were applied outside the winter season, returning the strength of the subtropical jet to normal values. However, air temperatures over the North Atlantic and Europe in the summer season (June-August) are lower than in the control climate, with the largest difference over the North Atlantic (ca. 1.5°C) to ca. 0.5°C-1.0°C over Europe. We relate the decrease in summer temperatures largely to the thermal inertia of the ocean.

5 Conclusions and Discussion

The concept of triggering abrupt climate change by a repositioning of the North Atlantic eddy-driven jet avoids a number of problems associated with the traditional view of triggering rapid climate change (i.e. a meltwater pulse followed by a collapse of the MOC). In the alternative view, the Atlantic eddy-driven jet shifts from a southwest - northeast orientation to a zonally oriented position hugging the subtropical jet. Consequently, the atmospheric meridional heat transport into mid- and high-latitudes is drastically reduced. The repositioning of the eddy-driven jet follows an increase in subtropical jet strength, and in this study we calculated forcing patterns that lead to a stronger subtropical jet over the North Atlantic sector.

The simulations described here reproduce the transition of a double jet situation, with coexisting eddy-driven and subtropical jets, to a single jet situation, where eddy-driven and subtropical jet coincide, when the strength of the subtropical jet is increased. We conclude that this a robust feature of the atmosphere as it can also be modelled using a coarse resolution (T21, L3) quasi-geostrophic model.

Regarding possible mechanisms which relate to an increase in subtropical jet strength, SEAGER and BATTISTI (2007) argue that changes in the distribution and strength of tropical convection may be involved in reorganizing mid- and high-latitude atmospheric circulation. Indeed, climate records indicate that abrupt climate changes often coincide with changes in the tropical climate. The proposed mechanism involves a stronger Hadley circulation in cold periods, in response to enhanced tropical convection, leading to a stronger subtropical jet.

The present study may provide an alternative forcing mechanism of tropical climate on the North-Atlantic subtropical jet strength, given the similarity in tendency perturbations of EXP1 and EXP2 reported here. In this alternative hypothesis, the jet stream acts as a global waveguide (BRANSTATOR, 2002) in which patterns of variability are zonally oriented chains of anomalies. Because they are meridionally trapped and zonally elongated, patterns associated with this so-called circumglobal wave guide connect activity at points over large distances (BRANSTATOR, 2002). Over the North Atlantic sector, the circumglobal waveguide has a distinct north-south dipole structure in the upper troposphere and projects strongly onto the NAO. Hence the possibility that a NAO persistently in one phase may be related to persistent forcing outside the North Atlantic basin.

Interestingly, in studying the atmospheric response to a change in sea-surface temperatures in the tropical Atlantic, HAARSMA and HAZELEGER (2007) found both an upper-troposphere Rossby wave response, with its en-

Table 1: Experiments discussed in this study.

experiment	subtropical jet strengthened by	tendency perturbations applied during	max. speed of subtropical jet
EXP1	sharpening meridional gradient of streamfunction at 200hPa	whole year	45.1 m/s
EXP2	persistently negative NAO-pattern at 200 hPa	extended winter (December - March)	43.3 m/s

ergy trapped in the circumglobal waveguide, and a response on the Atlantic's Hadley circulation, leading to a stronger subtropical jet.

In closing it must be readily admitted that many aspects of the chain of events leading to rapid climate change are not included in this study. The most obvious are tropical SSTs and their effect on atmospheric circulation via changes in deep convection, which is beyond the reach of this simple quasi-geostrophic model. However, this study demonstrates the plausibility of SEAGER and BATTISTI's (2007) hypothesis and the relevance of 'capturing' the eddy-driven jet by a strengthened subtropical jet as the trigger for abrupt climate change in the North Atlantic region.

Acknowledgements

Discussions with Jan Barkmeijer and Frank Selten are greatly appreciated. We thank Andreas Sterl for translating the abstract into German. GvdS is funded by the Netherlands Organization for Scientific Research (NWO) through the joint UK-NL RAPID Climate Change programme.

References

BARKMEIJER, J., P. HOUTEKAMER, X. WANG, 1993: Validation of a skill prediction model. – Tellus **45A**, 424–434.

BARKMEIJER, J., T. IVERSEN, T. N. PALMER, 2003: Forcing singular vectors and other sensitive model structures. – Quart. J. R. Met. Soc. **129**, 2401–2423 (doi:10.1256/qj.02.126).

BRANSTATOR, G., 2002: Circumglobal Teleconnections, the Jet Stream Waveguide, and the North Atlantic Oscillation. – J. Climate **15**, 1893–1910.

BROECKER, W. S., 2006: Was the Younger Dryas Triggered by a Flood? – Science **312**, 1146–1148 (doi:10.1126/science.1123253)

GOOSSE, H., E. DELEERSNIJDER, T. FICHEFET, M. H. ENGLAND, 1999: Sensitivity of a global ocean-sea ice model to the parameterization of vertical mixing. – J. Geophys. Res. (Oceans) **104**, 13681–13695.

GOOSSE, H. T. FICHEFET, 1999: Importance of ice-ocean interactions for the global ocean circulation: a model study. – J. Geophys. Res. (Oceans), **104**, 23337–23355.

GOOSSE, H., F. M. SELTEN, R. J. HAARSMA, J. D. OPSTEEGH, 2002: A mechanism of decadal variability of the sea-ice volume in the Northern Hemisphere. – Climate Dyn. **19**, 61–83.

GRIP MEMBERS, 1993: Climatic instability during the last interglacial period recorded in the GRIP ice core. – Nature **364**, 203–207.

HAARSMA, R. J., W. HAZELEGER, 2007: Extra-tropical atmospheric response to equatorial Atlantic cold tongue anomalies. – J. Climate **20**, 2076–2091.

HELD, I. M., M. J. SUAREZ, 1978: A two level primitive equation atmosphere model designed for climate sensitivity experiments. – J. Atm. Sci. **35**, 206–229.

HOSKINS, B. J., 2003: Atmospheric processes and observations. – Phil. Trans. R. Soc. Lond. A **361**, 1945–1960.

HOSKINS, B. J., P. J. VALDES, 1990: On the Existence of Storm-Tracks. – J. Atm. Sci. **47**, 1854–1864.

JAMES, I. N., 1994: Introduction to Circulating Atmospheres. – Cambridge University Press, 422 pp.

JONES, P. D., T. JÓNSSON, T., D. WHEELER, 1997: Extension to the North Atlantic Oscillation using early instrumental pressure observations from Gibraltar and south-west Iceland. – Int. J. Climatol. **17**, 1433–1450.

LACARRA, J., O. TALAGRAND, 1988: Short-range evolution of small perturbations in a barotropic model. – Tellus **40A**, 81–95.

LEE, S., H.-K. KIM, 2003: The Dynamical Relationship between Subtropical and Eddy-Driven Jets. – J. Atm. Sci. **60**, 1490–1503.

MARSHALL, J., F. MOLTENI, 1993: Toward a dynamic understanding of planetary-scale flow regimes. – J. Atm. Sci. **50**, 1792–1818.

OORTWIJN, J., J. BARKMEIJER, 1995: Perturbations That Optimally Trigger Weather Regimes. – J. Atm. Sci. **52**, 3922–3944.

OPSTEEGH, J. D., R. J. HAARSMA, F. M. SELTEN, A. KATTENBERG, 1998: ECBILT: A dynamic alternative to mixed boundary conditions in ocean models. – Tellus **50 A**, 348–367.

RÖHLING, E. J., H. PÄLIKE, 2005: Centennial-scale climate cooling with a sudden cold event around 8,200 years ago. – Nature **434**, 975–979.

RUTI, P. M., V. LUCARINI, A. DELL'AQUILA, S. CALMANTI, A. SPERANZA, 2006: Does the subtropical jet catalyze the midlatitude atmsopheric regimes? – Geophys. Res. Lett. **33**, L06814, (doi:10.1029/2005GL024620).

SEAGER, R., D. S. BATTISTI, 2007: Challenges to our understanding of the general circulation: abrupt climate change. – In: Schneider, T. and A. S. Sobel, (eds.), *The General Circulation of the Atmsophere*, (in press). Princeton University Press.

SEAGER, R., D. S. BATTISTI, J. YIN, N. GORDON, N. NAIK, A. C. CLEMENT, M. A. CANE, M. A., 2002: Is

the Gulf Stream responsible for Europe's mild winters? – Quart. J. R. Met. Soc. **128**, 2563.

SELTEN, F. M., R. J. HAARSMA, J. D. OPSTEEGH, 1999: On the mechanism of North Atlantic decadal variability. – J. Climate **12**, 1956–1973.

TAYLOR, K. C., C. U. HAMMER, R. B. ALLEY, H. B. CLAUSEN, D. DAHL-JENSEN, A. J. GOW, N. S. GUNDESTRUP, J. KIPFSTUHL, J. C. MOORE, E. D. WADDINGTON, 1993: Electrical conductivity measurements from the GISP2 and GISP Greenland ice cores. – Nature **366**, 549–552.

TRENBERTH, K. E., J. M. CARON, 2001: Estimates of Meridional Atmosphere and Ocean Heat Transports. – J. Climate **14**, 3433–3443.

VAN DER SCHRIER, G., J. BARKMEIJER, 2005: Bjerknes' hypothesis on the coldness during 1790-1820 AD revisited. – Climate Dyn. **24**, 355–371 (doi:10.1007/s00382-004-0506-x) Erratum: Climate Dyn. doi:10.1007/s00382-005-0053-0.

VAN DER SCHRIER, G., J. BARKMEIJER, 2007: The North American 1818-1824 drought and 1825-1840 pluvial and their relation to the atmospheric circulation. – J. Geophys. Res. (Atmospheres) **112**, D13102, doi:10.1029/2007JD008429.

VELLINGA, M., R. A. WOOD, 2002: Global Climatic Impacts of a Collapse of the Atlantic Thermohaline Circulation – Climatic Change **54**, 251–267.